

齿轮泵困油径向力的研究与量化分析

孙付春¹ 李玉龙^{2*} 钟飞¹

(1. 成都大学 机械工程学院,成都 6101060;

2. 宿迁学院 机电工程学院,江苏 宿迁 22380)

摘要 针对齿轮泵现有径向力计算的局限性问题,采用困油压力影响径向力的定量分析法,在1个困油周期内,先对从动轮齿顶圆上吸压、过渡、排压和困油的4区段内的动态液压分布,后基于实例困油压下的困油径向力进行研究和间接验证。结果表明:1)排压、吸压、过渡卸载下困油径向力的改善率分别为9.9%、-10.2%、-1.1%,困油压能改善排压卸载下的径向力,不过却恶化了吸压卸载下的径向力,对过渡卸载下径向力的影响不大,实际应用中,应尽量采用排压卸载的径向力减少措施;2)排压、吸压、过渡卸载下困油压力的冲击率分别为24.5%、38.5%和13.8%,对径向力的冲击很大,一方面要求通过卸荷槽创新尽量释放困油压力,另一方面应采用困油径向力的定量计算方法;3)困油压力对径向力的影响不仅在于本身更在于径向力的卸载措施,困油力由困油压力和作用面积共同决定,困油压、径向力、困油力的极值位置并非完全一致。困油径向力的定量计算方法为泵尤其是轴承的全流体润滑设计提供了动态的外载荷依据。

关键词 齿轮泵; 困油压力; 径向力; 液压力; 喷合力

中图分类号 TH325;TH137.3

文章编号 1007-4333(2018)12-0131-07

文献标志码 A

Research and quantitative analysis of the radial force impacted by trapped-oil pressure in external gear pumps

SUN Fuchun¹, LI Yulong^{2*}, Zhong Fei¹

(1. College of Industrial Engineering, Chengdu University, Chengdu 610106, China;

2. School of Mechanical and Electrical Engineering, Suqian College, Suqian 223800, China)

Abstract To overcome the limitations of current static calculation method of radial force without trapped-oil pressure in gear pumps, a new quantitative method for the influence of trapped-oil pressure on dynamic radial force was built. In a trapped-oil cycle, the dynamic fluid pressure distribution of four pressure sections, suction oil, transition oil pressure, discharge oil and trapped-oil pressure, on driven addendum circle were investigated, and the dynamic trapped-oil radial force were then studied and verified indirectly. The results showed that: The first improvement rate of new trapped-oil radial force to current radial force released differently by discharge oil, suction oil and transition oil was 9.9%, -10.2% and -1.1%, respectively. Then the radial force could be improved under relief by discharge oil. However, it was intensified under relief by suction oil and weakly impacted under relief by transition oil. Therefore, the relief by discharge oil was highly recommended in practice; The second impact rate of new trapped-oil radial force to current radial force released differently by discharge oil, suction oil and transition oil was 24.5%, 38.5% and 13.8%, respectively. The radial force was strongly impacted by trapped-oil pressure, so it was necessary to release trapped-oil pressure by innovated relief groove, and the new quantitative method was recommended to radial force calculation; The third effect of trapped-oil pressure on radial force was not only itself but also more other radial force relief measures. The trapped-oil force was collectively determined by trapped-oil pressure and its action area, so the

收稿日期: 2018-03-26

基金项目: 北京卫星制造厂资助项目(20804);四川省自然科学重点资助项目(16ZA0382)

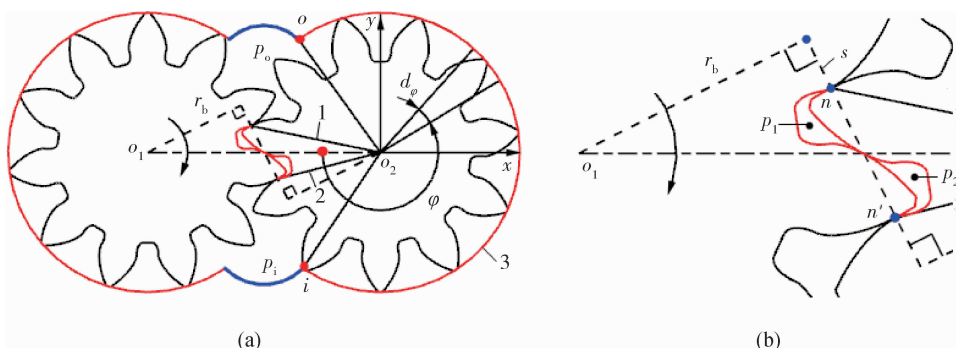
第一作者: 孙付春,副教授,主要从事农业机械基础研究与应用开发,E-mail:fch_sun@163.com

通讯作者: 李玉龙,教授,主要从事泵理论及现代设计方法研究,E-mail:leo-world@163.com

extreme position of trapped-oil pressure, radial force and trapped-oil force was not completely consistent. In conclusion, the calculation results of the new quantitative method provided an accurate external load for full fluid lubrication design of bearings and other

Keywords gear pumps; trapped-oil pressure; radial force; liquid force; meshing force

外啮合齿轮泵(简称齿轮泵)是一种泵送油液的动力元件,广泛应用于机床、冶金、轻工、建筑、船舶、飞机、汽车、石化等机械产品^[1-3],但由该泵结构所决定的困油现象的危害极其严重^[4],所造成急剧升高的困油压力,会引起轴-轴承等很大的冲击载荷^[5-6],并引起振动^[7-9]、噪声与气蚀^[10-13]、流量脉动^[14-15]等。针对困油现象的预防措施,目前主要涉及到尺寸优化和结构创新2个方面^[16-18],尤其是卸荷槽的结构创新^[19-22]。不过,在目前由啮合力和从动齿顶圆上的液压力所合成的径向力研究方面,除针对困油压力对啮合力的量化分析外^[23-24],采用的仍是静态的、过渡区液压力线性分布的传统方法^[10,25-26]。本研究旨在建立时变困油压力与从动轮上瞬态径向力的关系,以期获得困油压力影响径向力的量化结果,为泵尤其是轴承的全流体润滑设计,提供动态的外载荷依据。



1. 困油区起始边; 2. 困油区终止边; 3. 从动轮齿顶圆。

1. Starting edge of trapped-oil area; 2. Termination edge of trapped-oil area; 3. Addendum circle of driven gear.

o_1, o_2 为主、从动轮心; p_i, p_o 为吸、排油压, MPa, 图2同; p_1, p_2 为偏主、从轮一侧的困油压, MPa, 图3同; n 和 n' 为两个啮合点; i, o 为吸、排油腔轮廓与从动轮齿顶圆的交点; r_b 为基圆半径, mm; φ 为从动轮齿顶圆周上的任一位置角, rad, 图2同; x 和 y 为以从动轮心为原点的固定坐标轴; s 为主动齿面上啮合点 n 的曲率半径, mm, 图3和图4同。

o_1 and o_2 are the two circle centers of driving gear and driven gear; p_i and p_o are suction oil pressure and discharge oil pressure, MPa, similarly hereinafter in Fig. 2; p_1 and p_2 are the two trapped-oil pressures differently closed to driving gear and driven gear, MPa, similarly hereinafter in Fig. 3; n and n' are the two contact points; i and o are the two intersection points of driven addendum circle and suction cavity profile and discharge cavity profile; r_b is base circle radius, mm; φ is any position angle of driven addendum circle, rad, similarly hereinafter in Fig. 2; x and y are the two fixed axis from the driven center; s is corresponding curvature radius of driving profile in contact point, mm, similarly hereinafter in Fig. 3 and Fig. 4.

图1 从动轮齿顶圆周上的某一点位置(a)和困油区域放大图(b)

Fig. 1 A position on driven addendum circle (a) and enlarged figure of trapped-oil area (b)

1 困油液压力的圆周分布

图1示出具有相同齿形参数的主、从动齿轮的无(小)侧隙传动,轮心分别记为 o_1, o_2 , 以下以 o_1, o_2 分别代表主、从动齿轮。

设啮合点 n 在 o_1 工作齿面上的曲率半径为 s , 并以此作为动态的位置变量; 且以 o_1 上的前一个啮合点 n' 退出啮合,下一个齿顶点进入啮合的1个基节过程,作为1个困油周期,则^[4-5]

$$s \in [r_b \tan \alpha_a - p_b, r_b \tan \alpha_a] \quad (1)$$

式中: p_b 为基节, mm; r_b 为基圆半径, mm; α_a 为齿顶圆压力角, rad。它们均为齿形参数的函数^[13-15]。

在图1(b)所示的困油区内,无论是单齿啮合,还是双齿啮合,困油压力都是存在的^[4],记分别偏向 o_1, o_2 侧的两困油区内的介质压力为 p_1, p_2 。

记泵吸、排油腔与从动齿顶圆的交点为 i, o ; 设线段 io_2, oo_2 , 困油区起始边 1、困油区终止边 2 与中心线 $o_1 o_2$, 按 o_2 的逆时针方向所形成的圆心角分别为 $\varphi', \varphi'', \varphi_k', \varphi_k''$; φ 为图 1(a) 中以 $o_1 o_2$ 为起始边的 o_2 齿顶圆周上任一点所对应的圆心角; 过渡区起始角和终止角分别为 φ', φ'' 。则可将 o_2 齿顶圆分成如下的 4 个区段(图 2):

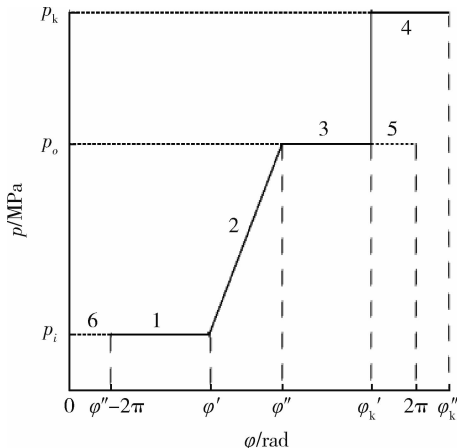
1) 吸压区段 1。由困油区终止边 2 和 $o_2 i$ 边形成, 受吸压 p_i 作用, 对应的吸压角为 $\varphi' - \varphi'' + 2\pi, \text{rad}$ 。

2) 过渡区段 2。由 $o_2 i$ 边和 $o_2 o$ 边形成, 受线性液压作用, 对应的过渡角为 $\varphi'' - \varphi', \text{rad}$ 。

3) 排压区段 3。由 $o_2 o$ 边和困油起始边 1 形成, 受排压 p_o 作用, 对应的排压角为 $\varphi_k' - \varphi'', \text{rad}$ 。

4) 困油区段 4。由困油起始边 1 与终止边 2 形成, 分别受 p_1, p_2 作用, 对应的困油角为 $\varphi_k'' - \varphi_k', \text{rad}$ 。

综上, 静态无困油径向力的计算区间为 $[0, 2\pi]$ 的吸压“6+1”、过渡 2、排压“3+5”的 3 区段构成; 动态困油径向力的计算区间则为 $[\varphi'' - 2\pi, \varphi'']$ 的吸压 1、过渡 2、排压 3、困油 4 的 4 区段构成。



1. 吸压区段; 2. 过渡区段; 3. 排压区段; 4. 困油区段; 5. 排压侧无困油区段; 6. 吸压侧无困油区段

1. Suction oil section; 2. Transition oil section; 3. Discharge oil section; 4. Trapped-oil section; 5. No trapped-oil section in discharge side; 6. No trapped-oil section in suction side

p_k, p 为困油压, 从动齿顶圆周上的分布压; $\varphi', \varphi'', \varphi_k', \varphi_k''$ 为图 1(a) 中线段 io_2, oo_2 , 困油边 1, 困油边 2 与 $o_1 o_2$ 所形成的圆心角。

p_k and p are trapped-oil pressure, distribution pressure on driven addendum circle; $\varphi', \varphi'', \varphi_k'$ and φ_k'' are the angles between center line differently and io_2, oo_2 and trapped-oil edge 1, trapped-oil edge 2 in Fig. 1(a).

图 2 从动轮齿顶上困油与无困油时的圆周液压力分布

Fig. 2 Fluid pressure distribution lines on driven addendum circle with or without trapped-oil pressure

2 径向力中的困油液压力

在式(1)所示的 1 个困油过程中, 先后所经过的 7 个特殊点位所对应的 s 分别为 $s_1 \sim s_7$ 。其中^[4,24]: $s_1 = r_b \tan \alpha_a - p_b; s_2 = 0.5L - 0.25p_b; s_3 = 2s_2 - s_1; s_4 = 2s_2 - s_0; s_5 = s_2 + 0.5p_b; s_7 = s_0 + p_b; s_7 = s_1 + p_b$ 。式中: L 为啮合线长度, mm; $s_0 = L - r_b \cos \alpha'$ ^[4,24]。

由 $s \in [s_1, s_7]$, 则 φ_k' 和 φ_k'' 分别为^[4]

$$\begin{aligned} \varphi_k'(s) &= \begin{cases} \varphi_{n1} & s \in [s_1, s_3] \\ \varphi_{c2} & s \in [s_3, s_6] \\ \varphi_{n2} & s \in [s_6, s_7] \end{cases} \\ \varphi_k''(s) &= \begin{cases} \varphi_{c1} & s \in [s_1, s_4] \\ \varphi_{n1} & s \in [s_4, s_7] \end{cases} \end{aligned} \quad (2)$$

式中:

$$\left. \begin{aligned} \varphi_{n1}(s) &= 2\pi - \{\arctan[(L-s)/r_b] - \alpha'\} \\ &\quad s \in [s_1, s_7] \\ \varphi_{c1}(s) &= 2\pi - \{\alpha' - \arctan[(s+0.5p_b)/r_b]\} \\ &\quad s \in [s_1, s_4] \\ \varphi_{n2}(s) &= 2\pi - \{\arctan[(L-s+p_b)/r_b] - \alpha'\} \\ &\quad s \in [s_6, s_7] \\ \varphi_{c2}(s) &= 2\pi - \{\alpha' - \arctan[(s-0.5p_b)/r_b]\} \\ &\quad s \in [s_3, s_7] \end{aligned} \right\} \quad (3)$$

图 1 中, 由 $\varphi \in [\varphi_k', \varphi_k'']$, 得

$$p_k(s, \varphi) = \begin{cases} p_1 & s \in [s_1, s_3] \\ p_2 & \varphi \in [\varphi_k', \varphi_{n1}) \\ p_1 & \varphi \in [\varphi_{n1}, \varphi_k''] \\ p_2 & s \in [s_4, s_6] \\ p_1 & \varphi \in [\varphi_k', \varphi_{c2}) \\ p_2 & \varphi \in [\varphi_{c2}, \varphi_k''] \end{cases} \quad (4)$$

式中: p_k 为困油压, MPa。则

$$p(s, \varphi) = \begin{cases} p_i & \varphi \in [\varphi_k'' - 2\pi, \varphi'] \\ p_i + \frac{p_o - p_i}{\varphi'' - \varphi'}(\varphi - \varphi') & \varphi \in [\varphi', \varphi''] \\ p_o & \varphi \in [\varphi'', \varphi_k'] \\ p_k & \varphi \in [\varphi_k', \varphi_k''] \end{cases} \quad (5)$$

式中: p 为从动轮齿顶圆周上的分布压, MPa。图 1(a) 的 φ 终止边处, 取一个角度为 $d\varphi$ 、厚度为 b 的微分区域, 则其表面积为 $dA = br_a d\varphi$, 作用该 dA 上的力

为 $dF_p = pdA = pbr_a d\varphi$ 。则

$$\left. \begin{aligned} dF_{px} &= pbr_a \cos\varphi d\varphi \\ dF_{py} &= pbr_a \sin\varphi d\varphi \end{aligned} \right\} \quad (6)$$

式中: dF_{px} 、 dF_{py} 为 dF_p 的 x 、 y 轴分力,N; r_a 为顶圆半径,mm; b 为齿宽,mm。由式(6)的积分,得

$$\left. \begin{aligned} F_{px}(s) &= br_a(A_x + \\ &\quad \int_{\varphi_k''-2\pi}^{\varphi_k''} p(s, \varphi) \cos\varphi d\varphi) = \\ &\quad br_a(A_x + B_x) \\ F_{py}(s) &= br_a(A_y + \\ &\quad \int_{\varphi_k''-2\pi}^{\varphi_k''} p(s, \varphi) \sin\varphi d\varphi) = \\ &\quad br_a(A_y + B_y) \end{aligned} \right\} \quad (7)$$

式中: F_{px} 、 F_{py} 为 x 、 y 轴上的液压分力,N。系数分别为:

$$\left. \begin{aligned} A_x &= p_i(\sin\varphi'' - \sin\varphi_k'') + p_o(\sin\varphi_k' - \sin\varphi'') + \\ &\quad (p_o - p_i)[\sin\varphi'' + (\cos\varphi'' - \cos\varphi')/(\varphi'' - \varphi')] \\ A_y &= p_i(\cos\varphi_k'' - \cos\varphi'') + p_o(\cos\varphi'' - \cos\varphi_k') + \\ &\quad (p_o - p_i)[- \cos\varphi'' + (\sin\varphi'' - \sin\varphi')/(\varphi'' - \varphi')] \end{aligned} \right\} \quad (8)$$

$$\left. \begin{aligned} B_x &= \begin{cases} p_1(\sin\varphi_k'' - \sin\varphi_k') & s \in [s_1, s_3] \\ p_2(\sin\varphi_{n1} - \sin\varphi_k') + \\ p_1(\sin\varphi_k'' - \sin\varphi_{n1}) & s \in [s_3, s_4] \\ p_2(\sin\varphi_k'' - \sin\varphi_k') & s \in [s_4, s_6] \\ p_1(\sin\varphi_{c2} - \sin\varphi_k') + \\ p_2(\sin\varphi_k'' - \sin\varphi_{c2}) & s \in [s_6, s_7] \\ p_1(\cos\varphi_k'' - \cos\varphi_k') & s \in [s_1, s_3] \\ p_2(\cos\varphi_{n1} - \cos\varphi_k') + \\ p_1(\cos\varphi_k'' - \cos\varphi_{n1}) & s \in [s_3, s_4] \\ p_2(\cos\varphi_k'' - \cos\varphi_k') & s \in [s_4, s_6] \\ p_1(\cos\varphi_{c2} - \cos\varphi_k') + \\ p_2(\cos\varphi_k'' - \cos\varphi_{c2}) & s \in [s_6, s_7] \end{cases} \\ B_y &= - \begin{cases} p_1(\cos\varphi_k'' - \cos\varphi_k') & s \in [s_1, s_3] \\ p_2(\cos\varphi_{n1} - \cos\varphi_k') + \\ p_1(\cos\varphi_k'' - \cos\varphi_{n1}) & s \in [s_3, s_4] \\ p_2(\cos\varphi_k'' - \cos\varphi_k') & s \in [s_4, s_6] \\ p_1(\cos\varphi_{c2} - \cos\varphi_k') + \\ p_2(\cos\varphi_k'' - \cos\varphi_{c2}) & s \in [s_6, s_7] \end{cases} \end{aligned} \right\} \quad (9)$$

如不考虑困油压力,则将 $B_x = B_y = 0$ 和 $\varphi_k'' = \varphi_k' = 2\pi$ 代入式(7)~(9),得

$$\left. \begin{aligned} F_{px}' &= br_a A_x \\ F_{py}' &= br_a A_y \end{aligned} \right\} \quad (10)$$

式中: F_{px}' 、 F_{py}' 为无困油液压力的 x 、 y 轴分力,N; 与文献[26]给出的公式完全一致。则

$$\left. \begin{aligned} F_p(s) &= \sqrt{F_{px}^2(s) + F_{py}^2(s)} \\ F_p' &= \sqrt{F_{px}'^2 + F_{py}'^2} \end{aligned} \right\} \quad (11)$$

式中: F_p 、 F_p' 分别为动态困油液压力和静态无困油液压力,N。

3 径向力中的困油啮合力

困油卸荷时,文献[24]给出了主、从动轮上的动态转矩式 $M_1(s, p_1, p_2)$ 、 $M_2(s, p_1, p_2)$,这里直接采用,由

$$F_t(s) = M_2(s, p_1, p_2)/r_b$$

式中: F_t 为困油啮合力,N。而文献[26]给出的为

$$F_t' = 0.5b(p_o - p_i)(r_a^2 - r'^2)/r$$

式中: F_t' 为无困油啮合力,N; r 、 r' 为分度圆、节圆半径,mm。得

$$\left. \begin{aligned} F_{tx} &= F_t \sin\alpha' \\ F_{ty} &= -F_t \cos\alpha' \\ F_{tx}' &= F_t' \sin\alpha' \\ F_{ty}' &= -F_t' \cos\alpha' \end{aligned} \right\} \quad (12)$$

式中: F_{tx} 、 F_{ty} 和 F_{tx}' 、 F_{ty}' 为 F_t 和 F_t' 的 x 、 y 轴分量,N。则

$$\left. \begin{aligned} F_r &= \sqrt{(F_{px} + F_{tx})^2 + (F_{py} + F_{ty})^2} \\ F_r' &= \sqrt{(F_{px}' + F_{tx}')^2 + (F_{py}' + F_{ty}')^2} \end{aligned} \right\} \quad (13)$$

式中: F_r 、 F_r' 分别为困油径向力、无困油径向力,N。

4 困油压力的仿真与拟合

文献[27]和[28]给出了计算 $p_1(s)$ 和 $p_2(s)$ 的仿真方法,这里直接采用。原始参数取 $p_o = 3$ MPa, $p_i = 0.1$ MPa, 转速 1 000 r/min; 模数 2, 齿数 11, 齿顶高系数 1.2, 顶隙系数 0.15, 压力角 $\alpha = 20^\circ$, 喷射角 $\alpha' = 27.12^\circ$, 齿宽 $b = 19.5$ mm。

由文献[5]知, $\max(p_1)$ 和 $\max(p_2)$ 发生在卸荷槽关闭点即 s_2 和 s_5 的附近^[5,13], 且 $\max(p_2) > \max(p_1)$ 。依据困油压力的仿真结果^[4-5,13,27-28], $p_1(s)$ 和 $p_2(s)$ 的多段拟合曲线如图 3 所示。

5 实例运算和间接验证

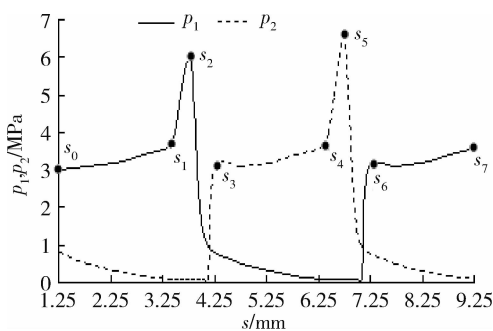
目前该泵的径向力卸载措施^[26], 可采用排压卸载, 取 $\varphi' = 30^\circ$ 和 $\varphi' = 96^\circ$; 或采用吸压卸载, 取 $\varphi = 264^\circ$ 和 $\varphi' = 330^\circ$; 或吸排压的过渡卸载, 取 $\varphi' = 30^\circ$ 和 $\varphi' = 330^\circ$ 。

在图 3 所示的困油压力和对应的泵原始参数下, 排压、吸压、过渡卸载下的动态困油径向力和静态无困油径向力结果见表 1 和图 4, 其中, 改善率和冲击率的定义为:

$$\text{改善率} = \left(1 - \frac{\text{困油径向力均值}}{\text{无困油径向力均值}}\right) \times 100\%$$

$$\text{冲击率} = \frac{\text{困油径向力最大值} - \text{困油径向力最小值}}{\text{无困油径向力均值}} \times$$

$$100\%$$



$s_1 \sim s_7$ 为 $[s_1, s_7]$ 困油区间内先后经过 7 个特殊点的位置变量; 图 4 同。

$s_1 \sim s_7$ are the seven special ordinal positions in a oil trapping process; Similarly hereinafter in Fig. 4.

图 3 1 个困油周期内偏主、从动轮侧的

2 困油压力拟合结果

Fig. 3 Two fitting polynomial curves of trapped-oil pressures differently closed to driving gear and driven gear in a trapped-oil process

排压、吸压、过渡卸载下的困油改善率分别为 9.9%、-10.2%、-1.1%。因此, 困油力能改善排压卸载下的径向力, 不过却恶化了吸压卸载下的径向力, 对过渡卸载下径向力的影响不大。其中, 无困油径向力的计算与文献[26]和[29]经验证的计算结果一致, 且由 $B_x = B_y = 0$ 和 $\varphi_k'' = \varphi_k' = 2\pi$ 下的困油径向力式(10)与文献[26]的完全一致, 说明困油径向力计算的准确性。

文献[29]由测试出的滑动轴承偏心距, 得出径向力降低 20%~30%, 轴承寿命提高 2.1~2.3 倍, 由此看出, 排压卸载下的困油压力能降低 9.9% 的径向力, 实际应用中, 应优先采用排压卸载措施。

排压、吸压、过渡卸载下困油压力的冲击率分别为 24.5%、38.5% 和 13.8%, 对径向力的冲击影响很大。其中, 吸压卸载下的峰值增加了 34.3% ($1239/922.8 - 1$), 而困油压力又被卸荷槽的卸荷能力所决

表 1 排压、吸压、过渡卸载下径向力的最大值、最小值、均值、改善率和冲击率

Table 1 Maximum, minimum, mean, improvement percent, and extreme volatility percent of radial force differently released by discharge oil, suction oil and transition oil

径向力 Radial force	最大值/N Maximum	最小值/N Minimum	均值/N Mean	改善率/% Improvement percent	冲击率/% Volatility percent
$F_{r,1}$	851.8	644.8	760.2	9.9	24.5
$F_{r,2}$	1 239.0	883.6	1 016.9	-10.2	38.5
$F_{r,3}$	1 180.0	1 031.6	1 088.9	-1.1	13.8
$F_{r,1}'$	843.4	843.4	843.4	—	—
$F_{r,2}'$	922.8	922.8	922.8	—	—
$F_{r,3}'$	1 076.9	1 076.9	1 076.9	—	—

注: $F_{r,1}, F_{r,2}, F_{r,3}$ 和 $F_{r,1}', F_{r,2}', F_{r,3}'$ 分别为排压、吸压、过渡卸载下的困油径向力和无困油径向力; 图 4 同。

Note: $F_{r,1}, F_{r,2}, F_{r,3}$ and $F_{r,1}', F_{r,2}', F_{r,3}'$ are three dynamic trapped-oil radial forces and three static current radial forces differently released by discharge oil, suction oil, transition oil. The same as in Fig. 4.

定, 这与文献[30]给出的卸荷槽改进后径向力(即无困油径向力)最大值, 降为改进前的 51%, 考虑到原始参数条件的不同, 趋势完全一致; 且由图 1 可以看出, 困油压力被限制在中心线两侧狭小的困油区间内, 与文献[30]的困油现象加剧径向力主要表现在两齿轮中心线方向的分力上的结论完全一致。

图 3 中, p_1 和 p_2 的最大峰值位置为 s_2 和 s_5 ; 而图 4 中, 排压卸载下的径向力却在该两位置处产生

的偏偏是最小峰值, 其最大峰值反而出现在 s_3 和 s_6 位置, 其他卸载措施下亦如此。这说明困油压力的极值位置并非一定是径向力的极值位置, 由此得出困油压力之于径向力的影响不仅在于本身更在于径向力的卸载措施。另外, 排压卸载下的径向力在 s_4 附近也出现一个局部极小值, 说明困油力为困油压力与其作用面积(或困油角)所共同决定, 由此得出困油压力的极值位置并非一定是困油力的极值位置。

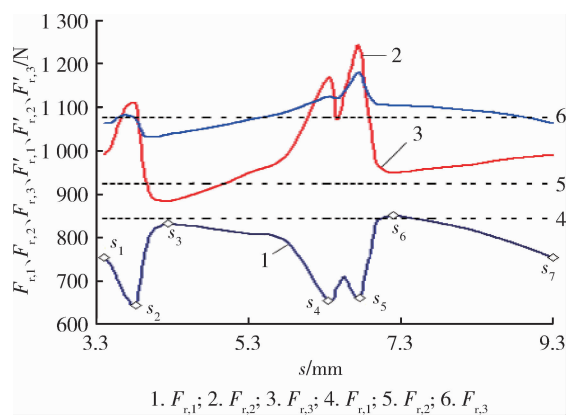


图4 1个困油周期内排压、吸压、过渡卸载下的困油径向力和无困油径向力

Fig. 4 Three new trapped-oil radial forces and three current radial force lines differently released by discharge oil, suction oil and transition oil in a trapped-oil process

6 结 论

1) 排压、吸压、过渡卸载下困油径向力的改善率分别为9.9%、-10.2%、-1.1%，困油能改善排压卸载下的径向力，但却恶化了吸压卸载下的径向力，对过渡卸载下径向力的影响不大。实际应用中，应尽量采用排压卸载的径向力减少措施。

2) 排压、吸压、过渡卸载下困油压力的冲击率分别为24.5%、38.5%和13.8%，对径向力的冲击很大。一方面要求由卸荷槽创新尽量释放困油压力，另一方面应采用困油径向力的计算方法。

3) 困油压力对径向力的影响不仅在于本身更在于径向力的卸载措施，困油力由困油压力和作用面面积共同决定，困油压力、径向力、困油力的极值位置并非完全一致。

参考文献 References

- [1] Devendran R S, Vacca A. Optimal design of gear pumps for exhaust gas aftertreatment applications [J]. *Simulation Modelling Practice & Theory*, 2013, 38(38):1-19
- [2] Osiński P, Deptula A, Partyka M A. Discrete optimization of a gear pump after tooth root undercutting by means of multi-valued logic trees [J]. *Archives of Civil & Mechanical Engineering*, 2013, 13(4):422-431
- [3] Devendran R S, Vacca A. A novel design concept for variable delivery flow external gear pumps and motors [J]. *International Journal of Fluid Power*, 2014, 15(3):121-137
- [4] 李玉龙. 外啮合齿轮泵困油机理、模型及试验研究[D]. 合肥: 合肥工业大学, 2010
- [5] Li Y L. Mechanism, modeling and experiment investigation of trapped oil in external gear pump[D]. Hefei: Hefei University of Technology, 2010 (in Chinese)
- [6] 李玉龙. 齿轮泵最大困油压力解析式的建立与验证[J]. 农业工程学报, 2013, 29(11):71-77
- [7] Li Y L. Establishment and verification of analytic formula for maximum trapped-oil pressure in external gear pump [J]. *Transactions of the Chinese Society of Agricultural Engineering*, 2013, 29(11): 71-77 (in Chinese)
- [8] Mucchi E, Dalpiaz G, Rincón A F D. Elastodynamic analysis of a gear pump. Part I: Pressure distribution and gear eccentricity[J]. *Mechanical Systems & Signal Processing*, 2010, 24(7):2160-2179
- [9] Mucchi E, Dalpiaz G, Rivola A. Elastodynamic analysis of a gear pump. Part II: Meshing phenomena and simulation results[J]. *Mechanical Systems & Signal Processing*, 2010, 24(7):2180-2197
- [10] Mucchi E, Dalpiaz G, Rincón A F D. Elasto-dynamic analysis of a gear pump-Part IV: Improvement in the pressure distribution modelling [J]. *Mechanical Systems & Signal Processing*, 2015, 50-51:193-213
- [11] Hemanth R. Design, modeling and analysis of a gear pump for dispensing application[J]. *Applied Mechanics & Materials*, 2014, 592-594:1035-1039
- [12] Fiebig W, Korzyb M. Vibration and dynamic loads in external gear pumps[J]. *Archives of Civil & Mechanical Engineering*, 2015, 15(3):680-688
- [13] Vacca A, Guidetti M. Modelling and experimental validation of external spur gear machines for fluid power applications [J]. *Simulation Modelling Practice & Theory*, 2011, 19(9):2007-2031
- [14] Mucchi E, Rivola A, Dalpiaz G. Modelling dynamic behaviour and noise generation in gear pumps: Procedure and validation[J]. *Applied Acoustics*, 2014, 77(77):99-111
- [15] 李玉龙. 外啮合齿轮泵困油膨胀区的最小压力[J]. 排灌机械工程学报, 2013, 31(12):1049-1055
- [16] Li Y L. The minimal trapped-oil pressure of expansion stage in external gear pump [J]. *Journal of Drainage and Irrigation Machinery Engineering*, 2013, 31 (12): 1049-1055 (in Chinese)
- [17] 李玉龙, 唐茂. 困油压力对齿轮泵流量脉动的影响分析[J]. 农业工程学报, 2013, 29(20):60-66
- [18] Li Y L, Tang M. Influence analysis of trapped oil pressure on flow pulsation in external gear pumps[J]. *Transactions of the Chinese Society of Agricultural Engineering*, 2013, 29(20): 60-66 (in Chinese)
- [19] 李玉龙, 刘春艳, 王生. 大侧隙外啮合齿轮泵的困油特性和流量特性[J]. 机械科学与技术, 2015, 34(3):454-458
- [20] Li Y L, Liu C Y, Wang S. The trapped oil characteristics and flow characteristics with large backlash gap in external

- gear pumps [J]. *Mechanical Science and Technology for Aerospace Engineering*, 2015, 34(3):545-548 (in Chinese)
- [16] Mucchi E, Dalpiaz G, Rivola A. Influence of design and operational parameters on the dynamic behavior of gear pump [J]. *Meccanica*, 2011, 46(6): 1191-1212
- [17] Wang S, Sakurai H, Kasarekar A. The optimal design in external gear pumps and motors [J]. *IEEE/ASME Transactions on Mechatronics*, 2011, 16(5):945-952
- [18] Tosi G, Mucchi E, D' Ippolito R, Dalpiaz G. Dynamic behavior of pumps: An efficient approach for fast robust design optimization[J]. *Meccanica*, 2015, 50(8):2179-2199
- [19] 李玉龙, 孙付春. 齿轮泵齿侧间隙与卸荷槽间距关系的定量分析[J]. 农业工程学报, 2012, 28(22):63-68
- Li Y L, Sun F C. Quantitative analysis of relationship between backlash value and distance of two relief grooves in external gear pump[J]. *Transactions of the Chinese Society of Agricultural Engineering*, 2012, 28 (22): 63-68 (in Chinese)
- [20] 李玉龙. 齿轮泵圆形卸荷槽下的困油压力分析[J]. 中国农业大学学报, 2014, 19(4):155-160
- Li Y L. Trapped-oil pressure analysis of gear pump with arc unloading groove [J]. *Journal of China Agricultural University*, 2014, 19(4):155-160(in Chinese)
- [21] 李玉龙, 孙付春, 唐茂. 高速齿轮泵渐开线型卸荷槽的设计与分析[J]. 机械科学与技术, 2014, 33(9):1377-1381
- Li Y L, Sun F C, Tang M. Design and analysis of the relief groove with involutes shape in the higher speed external gear pumps [J]. *Mechanical Science and Technology for Aerospace Engineering*, 2014, 33(9):1377-1381(in Chinese)
- [22] 李玉龙, 孙付春, 唐茂. 一种具有耳形卸荷槽的外啮合齿轮泵:中国, 10482913.7[P]. 2013-10-04
- Li Y L, Sun F C, Tang M. An external gear pump with an ear-shaped relief groove:China, 10482913.7[P]. 2013-10-04 (in Chinese)
- [23] 李玉龙, 刘焜, 王学军. 齿轮泵扭矩计算的动态再现[J]. 农业机械学报, 2006, 37(3):142-144
- Li Y L, Liu K, Wang X J. Dynamic reappearance on torque calculation in a gear pump with external mesh [J]. *Transactions of the Chinese Society for Agricultural Machinery*, 2006, 37(3):142-144(in Chinese)
- [24] 李玉龙, 刘焜. 考虑困油和卸荷的外啮合齿轮泵动态转矩计算[J]. 农业工程学报, 2009, 25(4):91-95
- Li Y L, Liu K. Calculation of dynamic torque acted on external gear pump considering relief groove and trapped oil pressure [J]. *Transactions of the Chinese Society of Agricultural Engineering* , 2009, 25(4):91-95 (in Chinese)
- [25] Luan, Z H. Research on synchronous gear pump [J]. *International Journal of Coal Science & Technology*, 2010, 16(4):429-433
- [26] 何存兴. 液压元件[M]. 北京:机械工业出版社,1982:53-63
- He C X. *Hydraulic Components*[M]. Beijing:China Machine Press,1982:53-63(in Chinese)
- [27] 李玉龙. 基于低速困油模型的外啮合齿轮泵高速困油特性分析[J]. 农业工程学报, 2012, 28(9):35-39
- Li Y L. Characteristic analysis of high-speed trapped-oil in external gear pump based on low-speed trapped-oil model[J]. *Transactions of the Chinese Society of Agricultural Engineering* , 2012, 28(9):35-39(in Chinese)
- [28] 李玉龙, 孙付春. 振动影响齿轮泵困油压力的仿真与理论分析[J]. 农业工程学报, 2012, 28(13):77-81
- Li Y L, Sun F C. Simulation and theoretical analysis on trapped oil pressure in external gear pump influenced by vibration [J]. *Transactions of the Chinese Society of Agricultural Engineering* , 2012, 28(13):77-81(in Chinese)
- [29] 那成烈, 纪洪年, 徐良, 梁勇. 现代高压齿轮泵的径向卸载[J]. 兰州理工大学学报, 1989,15(1):9-15
- Na C L, Ji H N, Xu L, Liang Y. Releasing of radial load in modern high-pressure gear pump[J]. *Journal of Lanzhou University of Technology* , 1989,15(1):9-15(in Chinese)
- [30] 冀宏, 赵光明. 基于流场的外啮合齿轮泵径向力计算[J]. 机床与液压, 2013,41(7):1-4
- Ji H, Zhao G M. Radial force calculation of external gear pump based on flow field[J]. *Machine Tool & Hydraulics* , 2013,41(7):1-4(in Chinese)

责任编辑: 刘迎春